UC Davis
UC Davis Previously Published Works

Title
Degradation of organic pollutants in/on snow and ice by singlet molecular oxygen (1 O *2) and an organic triplet excited state

Permalink
https://escholarship.org/uc/item/759225x2

Journal
Environmental Science Processes & Impacts, 16(4)

ISSN
2050-7887

Authors
Bower, Jonathan P
Anastasio, Cort

Publication Date
2014-04-01

DOI
10.1039/c3em00565h

Supplemental Material
https://escholarship.org/uc/item/759225x2#supplemental

Peer reviewed

eScholarship.org Powered by the California Digital Library
University of California

October 26, 2013

Degradation of organic pollutants in/on snow and ice by singlet molecular oxygen ($^1O_2$*) and an organic triplet excited state

Jonathan P. Bower[1] and Cort Anastasio[1,*]

[1]Department of Land, Air, and Water Resources
University of California, Davis
One Shields Avenue
Davis, CA 95616

*Corresponding address

Cort Anastasio
Land, Air, and Water Resources
University of California, Davis
One Shields Avenue
Davis, CA
Telephone: 530.754.6095
Fax: 530.752.1552
email: canastasio@ucdavis.edu

Submitted to Environmental Science: Processes & Impacts (October 26, 2013)

Abstract:

Singlet molecular oxygen ($^1O_2$*) can be a significant sink for a variety of electron-rich pollutants in surface waters and atmospheric drops. We recently found that $^1O_2$* concentrations are enhanced by up to a factor of 10^4 on illuminated ice compared to in the equivalent liquid solution, suggesting that $^1O_2$* could be an important oxidant for pollutants in snow. To examine this, here we study the degradation of three model organic pollutants: furfuryl alcohol (to represent furans), tryptophan (for aromatic amino acids), and bisphenol A (for phenols). Each compound was studied in illuminated aqueous solution and ice containing Rose Bengal (RB, a sensitizer for $^1O_2$*) and sodium chloride (to adjust the concentration of total solutes). The RB-mediated loss of each organic compound is enhanced on illuminated ice compared to in solution, by factors of 6400 for furfuryl alcohol, 8300 for tryptophan, and 50 for bisphenol A for ice containing 0.065 mM total solutes. Rates of loss of furfuryl alcohol and tryptophan decrease at a higher total solute concentration, in qualitative agreement with predictions from freezing-point depression. In contrast, the loss of bisphenol A on ice is independent of total solute concentration. Relative to liquid tests, the enhanced loss of tryptophan on ice during control experiments made with deoxygenated solutions and solutions in D_2O show that the triplet excited state of Rose Bengal may also contribute to loss of pollutants on ice.

1. Introduction

To understand the cycling and fate of organic pollutants in cold environments, a growing number of studies are examining the direct and indirect photoreactions of pollutants in/on ice. Direct photodegradation – where a pollutant absorbs light and is degraded – has been examined for PAHs,[1,2] PCBs,[3] phenols,[4] and pesticides[5] on ice. Other studies have examined indirect photodegradation, where a separate species absorbs light and forms a reactive intermediate that then reacts with the pollutant. For example, photolysis of hydrogen peroxide on ice forms hydroxyl radical ($^{\bullet}$OH), which can react with organic compounds.[6-8]

Another photo-formed oxidant that may participate in the indirect photodegradation of pollutants on ice is singlet molecular oxygen, $O_2(^1\Delta_g)$ (or, more simply, $^1O_2$*). As shown in scheme 1, the first step in singlet oxygen formation is light absorption by a sensitizer (such as chromophoric dissolved organic material, CDOM) and formation of an excited singlet state (^{1}CDOM*). A portion of this singlet state undergoes intersystem crossing (ISC) to the excited triplet state (^{3}CDOM*), which can transfer energy to dissolved oxygen, exciting it from ground state triplet oxygen to the higher-energy singlet state.[9-12] The CDOM triplet state can also react directly with a pollutant or decay to the ground state through processes such as phosphorescence.

In surface waters and cloud and fog drops $^1O_2$* is formed from illumination of natural CDOM[11,13-15] and can be a significant sink for furans,[10] amino acids,[16,17] and phenols.[18,19] On ice, freeze-concentration can produce levels of $^1O_2$* that are thousands of times higher than in the equivalent liquid solution with the same bulk composition.[20,21] Because of this enhancement, concentrations of $^1O_2$* in illuminated snow from California and Greenland are approximately 100 times greater than levels in illuminated polluted fog waters from the Central Valley of California,[14,21] even though light absorption by the snow is approximately 100-1000 times lower than in the fog.[22] These enhancements suggest $^1O_2$* could be an important oxidant in frozen samples for a variety of electron-rich organic compound classes.

The goal of this work is to explore whether the enhanced concentration of $^1O_2$* on ice might be important for the degradation of pollutants in illuminated snow and ice. To do this we measured the reaction kinetics of several organic compounds in illuminated liquid and ice samples containing Rose Bengal as a sensitizer for $^1O_2$* formation. We studied the decay of three organic pollutants - furfuryl alcohol, tryptophan, and bisphenol A – to represent furans, aromatic amino acids, and phenols, respectively. In each case we also conducted control experiments in both D_2O and in degassed solutions (to remove O_2) to isolate and identify the reactivity of the pollutants with $^1O_2$*.

2. Experimental Methods

Furfuryl alcohol (FFA, 99%), Rose Bengal (RB, ≥ 85%), 2-nitrobenzaldehyde (2NB, 98%) and sodium chloride (NaCl, 99.999%) were purchased from Sigma-Aldrich. Tryptophan (TRP, 98%), bisphenol A (BPA, 97%), and deuterium oxide (D_2O, 99.95%) were from Acros while acetonitrile (ACN, HPLC grade) was from Fisher. Purified water (Milli-Q, ≥18.2 MΩ cm) was obtained from a Milli-Q Plus system with an upstream Barnstead B-Pure cartridge to remove organics. All reagents were used as received and all solutions were air-saturated unless noted.

For ice experiments, we made solutions with a low concentration (10 to 50 nM) of pollutant (FFA, TRP, or BPA) and either 0.0325 or 3.0 mM NaCl to yield total solute (TS) concentrations of 0.065 and 6.0 mM, respectively. Liquid samples were prepared with 50 nM of pollutant and 0.0325 mM NaCl (0.065 mM TS). We have previously reported that the impact of changes in total solute concentration on $^1O_2$* formation in liquid solutions is very small: less than a factor of ~1.7 decrease in [$^1O_2$*] over a factor of 7.0 10^4 increase in total solute concentration.[20] We chose pollutant concentrations so that the pollutant was a minor sink for $^1O_2$* (i.e., accounting for < 30% of $^1O_2$* loss) and H_2O was the major sink; as described in Supplemental Section S1 this was only a concern in ice tests. The 0.065 mM TS concentration was selected to represent a remote, continental snow, while the 6.0 mM TS value was chosen to represent conditions in coastal snows with significant sea-salt inputs. We also chose the latter value because we have found that freezing-point depression (FPD) can describe $^1O_2$* kinetics on ice in

this TS region.[20] Rose Bengal was added as the sensitizer for $^1O_2$*, at a concentration of 100 nM for liquid tests and 10 nM for ice tests. After solutions were prepared, 720 µL aliquots were pipetted into ~1-mL custom-made, open-top, PTFE ice-pellet molds and placed in a covered, Peltier-cooled, freeze chamber at –10 ˚C for at least 1 hour to freeze.[21]

In some ice experiments we used D_2O instead of H_2O as the solvent as a diagnostic tool for $^1O_2$*. The room temperature rate constant for deactivation of $^1O_2$* in D_2O (k'_{D2O} = 1.6 × 10^4 s^{-1}; ref. 9) is 13.8 times lower than in H_2O (2.2 × 10^5 s^{-1}; ref. 9). Thus, because the solvent is the dominant sink for $^1O_2$* in solution, the steady-state concentration of $^1O_2$* is 13.8 times higher in D_2O compared to the equivalent sample in H_2O; the pseudo-first order rate constant for loss of a compound that reacts with singlet oxygen is similarly elevated in D_2O. As another diagnostic for $^1O_2$*, we conducted control experiments using degassed solutions to reduce dissolved O_2 in order to minimize $^1O_2$* concentrations in the illuminated samples. In these tests, 1.2 mL of solution was pipetted into a 2-mL glass vial, sealed with a septum-lined cap and purged with 99.998% N_2 (PraxAir) for 20 min. Sealed vials for ice tests were then frozen in a commercial freezer (–20˚C) for a minimum of 1 h. Ice experiments in vials containing solutions that were not degassed (i.e., the typical air-saturated samples) were also conducted.

Samples were illuminated with 549 nm light (a peak in RB absorbance) using a monochromatic illumination system with a 1000 W Hg/Xe lamp (Spectral Energy). Liquid tests were conducted at 5˚C in 2-cm quartz cuvettes (or 2-mL glass vials for degassed tests) while ice tests were conducted at –10 ˚C. All samples were given a minimum of 5 min to equilibrate to the temperature of the illumination chamber before illumination. No losses were observed in dark controls.

To control for daily variations in photon flux, actinometry experiments were conducted with 2-nitrobenzaldehyde (2NB) at 313 nm on each experiment day, as described previously [23]. Actinometry was performed in the same manner as the associated experiments: liquid in quartz cuvettes (or vials) at 5˚C and ice in ice-pellet molds (or vials) at –10˚C.

After illumination, samples were thawed at room temperature in the dark and then analyzed for pollutant concentration by HPLC (Shimadzu SPD-10A UV-Vis detector, LC-10AT pump, BetaBasic-18 column (Thermo Hypersil-Keystone), and 400 µL injection loop). Eluents (in Milli-Q) and detection wavelengths were: 10% ACN at 220 nm for FFA and TRP, 50% ACN at 240 nm for BPA, and 60% ACN at 258 nm for 2NB. Pseudo-first order rate constants for loss of the pollutant (k'_p) were determined from the slope of plots of $\ln([p]/[p]_0)$ versus illumination time, where $[p]$ and $[p]_0$ are the molar concentrations of FFA, TRP, or BPA at time t and t = 0, respectively. First-order rate constants for loss of 2NB (j_{2NB}) were determined in the same manner. Each pollutant decay rate constant was normalized to the daily value of j_{2NB}:

$$k_p^* = \frac{k_p}{j_{2NB}} \quad (1)$$

where k_p^* is the normalized apparent-first order rate constant for pollutant loss. Because 2NB loss is very slow with illumination at 549 nm (the wavelength of sample illumination), we used 313 nm light for the actinometry measurement. Because the photon fluxes at 313 and 549 nm are strongly correlated, the j_{2NB} data allow us to normalize sample kinetics for variations in photon flux.[20] Listed errors and error bars in this paper are ± 1 standard error, propagated from the standard errors of the measurements.

3. Results & Discussion

3.1. Pollutant loss in liquid and ice.

Table 1 compiles the structures, rate constants with singlet oxygen, and solubilities for our three model pollutants. Rate constants with $^1O_2$* are all quite high and are within a factor of approximately 2 of each other at 263 K, with a reactivity order of BPA ~ FFA > TRP. The room temperature water solubilities span a larger range, from miscible for FFA to 0.5 mM for BPA. The relative solubilities in liquid-like regions in/on ice at –10 ˚C are probably very similar to this order, but we were unable to find solubility data at low temperatures.

To characterize the decay kinetics of each model pollutant, we illuminated solutions and ice pellets and monitored the change in pollutant concentration over time. Figure 1 shows an example of the results, in this case for tryptophan. For both the liquid and ice samples there is direct photodegradation of TRP, but TRP loss is much faster in solutions containing Rose Bengal as a source of $^1O_2$*. Furthermore, even though RB concentrations are 10 times lower in ice samples compared to in the liquid samples, the loss of TRP in the presence of RB is dramatically faster on ice than in liquid, by factors of 600 and 12 for total solute concentrations of 0.065 and 6.0 mM TS, respectively. The slowing of TRP loss with increasing total solute (TS) concentration occurs for ice with and without RB (Figure 1B). This behavior for ice with RB (i.e., with a source of $^1O_2$*) is qualitatively what is expected based on freezing-point depression, as discussed below. However, the rate constant for direct photodegradation of TRP significantly decreased with increasing total solutes, which is unexpected: it could be because the direct photodegradation of TRP depends on the total solute level or because there is a trace contaminant in our samples that is a sensitizer for $^1O_2$*, as we previously observed for ice illuminated with simulated sunlight.[21] The main observations for TRP – that loss on ice is faster than in liquid, and that direct photodegradation is small compared to decay when RB is present – generally also extend to both FFA and BPA, although the observed rate constants for loss vary (Supplemental Figures S1 and S2).

From the slope of plots such as those shown in Figure 1, we calculate the photon-flux-normalized, pseudo-first-order rate constant for loss of each pollutant (Equation 1). In liquid solutions containing 100 nM RB, values of k^*_p for the three pollutants are within a factor of 2.5 (Figure 2A): $k^*_{FFA,LIQ} = 0.0011\ s^{-1}/s^{-1}$, $k^*_{TRP,LIQ} = 0.0019\ s^{-1}/s^{-1}$, and $k^*_{BPA,LIQ} = 0.0025\ s^{-1}/s^{-1}$. These correspond to pollutant lifetimes of 280 min for FFA, 150 min for TRP, and 120 min for BPA. These losses in the presence of RB (i.e., in the presence of $^1O_2$*) are much higher than direct photodegradation ("hν only") losses for FFA and BPA, by factors of 78 and 29, respectively. In contrast, direct photodegradation for TRP is significantly faster than for the other two organics and adding 100 nM RB only increases k^*_{TRP} by a factor of 3 in liquid solutions. Since there is no significant absorption of light at 549 nm by FFA,[10] TRP,[24] or BPA,[25] we expect little to no direct photodegradation of these pollutants. So the apparent direct photodegradation, particularly the relatively rapid loss of TRP, is puzzling. This evidence, together with the total solute dependence of direct photodegradation on ice (e.g., Figure 1B), further supports the idea that our samples contain a small amount of photoactive contaminant. However, with the exception of TRP, direct photodegradation in solution is minor compared to loss in the presence of RB (and thus $^1O_2$*). This result is also true for ice-phase experiments, as described below.

We also examined pollutant loss due to direct photodegradation and $^1O_2$* (i.e., in the presence of RB) in ice experiments at two different total solute concentrations (0.065 and 6.0 mM). Direct photodegradation is roughly the same for all of the pollutants in ice at both total solute levels, with an average (± 1 σ) value of 0.0011 (± 0.0004) s^{-1}/s^{-1}, with the exception of TRP in 0.065 mM TS ($k^*_{TRP,ICE,h\nu\ only} = 0.0091\ s^{-1}/s^{-1}$) (Figure 2B). The increase in direct photodegradation on ice compared to liquid for all pollutants could be due to red-shifting of their absorption spectra, which would increase light absorption by the pollutants at 549 nm; this shift has been observed for benzene in frozen samples.[26] Despite enhanced direct photodegradation on ice, this pathway is much slower than pollutant loss in frozen solutions containing 10 nM RB: k^*_p in the direct photodegradation experiment is always less than 10% of the value observed for ice containing RB and is often less than 1% (i.e., for both FFA cases and for TRP at 0.065 mM TS) (Figure 2B).

Pollutant loss in ice containing $^1O_2$* is much faster than in the companion liquid-phase tests, even with 10 times less sensitizer in the ice samples. For example, with 0.065 mM TS, k^*_p values on ice are 600 (TRP) and 640 (FFA) times faster than the corresponding liquid values, though enhancement of BPA loss on ice was only 6 times faster than in solution (Figure 2). The corresponding pollutant lifetimes for these ice samples with RB are 0.3 min for FFA, 0.2 min for TRP, and 13 min for BPA. For FFA and TRP, increasing the total solute concentration from 0.065 to 6.0 mM decreases the rate constant for pollutant loss in illuminated ice containing RB; in contrast, BPA loss is essentially the same at both total solute

values (Figure 2B). With 6.0 mM of total solutes, the pollutant lifetimes are 2 min for FFA, 8 min for TRP, and 16 min for BPA.

3.2 Effect of freezing-point depression on pollutant loss

The enhancement of k^*_p on ice relative to liquid, as well as the diminishing of k^*_p with increasing total solute concentration in ice, is consistent with solutes concentrating into liquid-like regions (LLRs) in the ice sample. If a solution is slowly frozen, most impurities are segregated from the ice to highly concentrated, liquid-like regions at the air-ice interface and at ice grain boundaries. In the frozen sample, the volume and composition of the LLRs can often be described by freezing-point depression (FPD).[27] The LLR volume in/on ice (V_{LLR}) is only a small fraction of the volume of the initial unfrozen solution (V_{LIQ}). Thus, for a solute "*m*" that is completely segregated from the ice into LLRs, the number of moles of *m* in the liquid and LLRs in the ice is the same, but the reduced LLR volume after freezing results in a concentration increase for *m*. This concentration enhancement of solutes in LLRs in/on ice relative to liquid values can be expressed by a freeze-concentration factor, *F*,[20,21]

$$F = \frac{V_{LIQ}}{V_{LLR}} = \frac{[m]_{LLR}}{[m]_{LIQ}} \approx \frac{T - T_f}{E_f [TS]} \quad (2)$$

where T is temperature, T_f is the temperature of fusion (i.e., melting temperature) of the pure solvent and E_f is the cryoscopic constant (1.86 K kg mol^{-1} for water).[28] Thus, *F* decreases with increasing total solute (TS) concentration in the initial liquid solution and with increasing ice temperatures. The concentration of $^1O_2$* is enhanced in LLRs of ice because the concentration of the singlet oxygen source (here RB) in LLRs is increased by a factor of *F* compared to the initial solution, while the concentration of the dominant sink for $^1O_2$* (i.e., water) remains essentially unchanged between solution and ice.[21]

We can use measurements of k^*_p in solution and ice to experimentally determine values of *F* in our experiments (F_{Exp}). To do this we subtract the contribution of direct photodegradation from pollutant loss in liquid and ice, and then take the ratio of the result on ice to that in liquid:

$$F_{Exp} = \frac{\left(k^*_{p,RB+h\nu} - k^*_{p,h\nu\ only}\right)_{LLR}}{0.10\left(k^*_{p,RB+h\nu} - k^*_{p,h\nu\ only}\right)_{LIQ}} \quad (3)$$

The factor of 0.10 scales the concentration of RB in the liquid experiments (100 nM) to the concentration used in ice tests (10 nM) (i.e., $[RB]_{ICE} = 0.10 \times [RB]_{LIQ}$); we have experimentally confirmed that k^*_p in liquid is directly proportional to [RB].[20]

Using equation 3 we calculated values of F_{Exp} based on our data from Figure 2. As shown in Figure 3, at 0.065 mM TS the losses of FFA and TRP are several thousand times faster on ice than liquid, with F_{Exp} values of 6400 and 8300, respectively. In contrast, the enhancement of BPA loss on ice was

much less pronounced, with a value of F_{Exp} of 57. The dramatic enhancements of pollutant loss in frozen samples, especially for FFA and TRP, highlight the potential importance of $^1O_2$* to pollutant decay on illuminated ice and snow.

At the higher total solute concentration of 6.0 mM the measured enhancement of FFA reactivity (F_{Exp} = 1000) closely matches the freeze-concentration factor predicted from freezing-point depression (Figure 3). In contrast, the enhancement of TRP reactivity (F_{Exp} = 150) at 6.0 mM TS is about six times lower than predicted by freezing-point depression. The suppressed enhancement for TRP loss compared to freezing-point depression is similar to what is observed for both FFA and TRP at 0.065 mM TS: values of F_{Exp} are approximately an order of magnitude lower than the value predicted by freezing-point depression (i.e., F_{FPD}), which is 82,000 (top dashed line in Figure 3). We have seen this experimental underestimation of the freeze-concentration factor predicted by freezing-point depression previously for FFA at low TS concentrations.[20]

Why is the experimental value of F_{Exp} for FFA at 0.065 mM TS lower than that predicted from freezing point depression (Figure 3)? Since FFA is miscible with water, we do not believe it is precipitating in the LLRs of our ice samples. The good agreement between F_{Exp} and F_{FPD} at 6.0 mM TS for FFA suggests that both FFA and RB remain soluble in LLRs (and that the reaction matrix is akin to liquid water), but at 0.065 mM TS the concentrations of solutes in LLRs are higher by a factor of 100. So at 0.065 mM TS it is possible that RB is precipitating or aggregating and thereby decreasing F_{Exp} from the expected value based on freezing-point depression. This same RB effect could be responsible for the lower value of F_{Exp} for TRP in/on 0.065 mM TS ice, but does not appear to explain the 6.0 mM TS TRP ice result since the 6.0 mM TS FFA ice result matches FPD (Figure 3).

We next consider the case of BPA, whose loss on ice is about 50 times higher than in liquid (after adjusting for differences in [RB]) at both 0.065 and 6.0 mM TS (Figures 3). While BPA loss is enhanced on ice, F_{Exp} for BPA in 0.065 mM TS samples is very similar to that observed at 6.0 mM TS and more than 3 orders of magnitude lower than predicted by freezing-point depression (Figure 3). With the lowest solubility of the three pollutants, and the lowest value of F_{Exp}, the evidence suggests BPA is precipitating in the ice samples. If this occurs, the measured rate constant for BPA loss would underestimate the loss occurring in the liquid-like regions because the measured value is influenced by the precipitated, likely non-reactive, portion of pollutant. Whether this occurs in natural ice and snows is unclear. Another possibility is that BPA is aggregating into hydrophobic microregions that are separate from the liquid-like phase of LLRs.[29] RB is a hydrophilic sensitizer, which implies that $^1O_2$* is formed in LLRs. If a hydrophobic, organic sub-phase exists within the LLRs (or bulk matrix) of our ice samples, it is possible that the photoformed $^1O_2$* is not collocated with much of the BPA, which would reduce the rate constant for BPA loss.

3.3 Diagnostic tests for $^1O_2$* on illuminated ice

To examine whether pollutant loss is primarily due to $^1O_2$* in our ice samples, we performed two diagnostic tests that are often used in solution studies of singlet oxygen. In the first, we degassed samples with N_2 to remove O_2 from the solution and then froze the solutions under N_2; under these low-O_2 conditions, the $^1O_2$* concentration in LLRs should be greatly suppressed, which will largely eliminate the $^1O_2$* pathway of pollutant loss. Figure 4 shows the ratio of k^*_p determined in an experiment with a degassed sample to that in a sample made from the standard, air-saturated solution; for both rate constants we subtract the small contribution from direct photodegradation (Figure S3) and normalize for variations in photon flux. In ice samples with 0.065 mM TS, removing O_2 greatly slows pollutant loss compared to loss in the air-saturated samples: rate constants for pollutant loss in the degassed ice are lower by 94 (± 2)% for FFA, 86 (± 3)% for TRP, and 90 (± 5)% for BPA. These results suggest that on ice with low total solute concentrations (and thus high *F* values) reaction with $^1O_2$* is the dominant loss pathway for the three organics. For ice made from 6.0 mM TS solutions, degassing reduces k^*_p in the air-saturated sample by 96 (± 9)% for FFA, 53 (± 11)% for TRP, and 80 (± 10)% for BPA. These results confirm that $^1O_2$* is the dominant sink for FFA and BPA on ice, but for TRP $^1O_2$* accounts for approximately half of the amino acid loss, indicating that one or more other reaction pathways are significant at 6.0 mM TS in the degassed ice sample. Degassing has the smallest effect on the rate constant of pollutant loss in liquid samples: compared to air-saturated samples, kinetics in degassed solutions are 66 (± 10)% lower for FFA, only 29 (± 14)% lower for TRP and essentially unaffected for BPA. While $^1O_2$* remains the dominant sink for FFA, for both TRP and BPA the loss in degassed liquid solutions is dominated by non-$^1O_2$* pathways.

Although our results in Figures 2, 3, and 4 are generally consistent with $^1O_2$* as the dominant oxidant for the pollutants, they also suggest that the excited triplet state of Rose Bengal (^{3}RB*) contributes to the enhanced pollutant loss we observe in/on ice. In air-saturated samples most ^{3}RB* will react with O_2, but in degassed samples the lack of O_2 will increase the potential reactions of ^{3}RB* with the pollutant (Scheme 1). Because O_2 is the dominant sink for ^{3}RB* in our air-saturated samples, eliminating O_2 will increase the steady-state concentration of ^{3}RB*, making it a more important sink for the pollutant. Based on past work,[30-32] the lifetime for the RB triplet state is approximately 3 μs in air-saturated solution (where O_2 is the dominant sink) and 130 μs in degassed solution (where unimolecular decay to the ground state is the dominant sink). Thus the steady-state concentration of ^{3}RB* will be higher by a factor of approximately 40 in the degassed samples compared to in the air-saturated samples (Supplemental Section S3). Therefore, a significant loss of a pollutant in degassed samples does not necessarily mean that ^{3}RB* was important in the air-saturated samples. As described in supplemental section S3, we can

use the degassed results to estimate f_{p+3RB*}, the fraction of pollutant loss that is due to reaction with RB triplets in the air-saturated samples.

We first consider the impact of degassing, and the resulting elevated triplet state concentration, on FFA decay. In the aqueous phase, FFA reportedly does not react appreciably with triplet excited states but does react rapidly with $^1O_2$*.[33] This is consistent with our FFA solution results. As shown in Figure 4, the ratio of $k^*_{p,degassed}/k^*_p$ is 0.34, but this value is high only because of the 40-fold increase in [^{3}RB*] due to degassing: as shown in the right-hand axis of Figure 4, ^{3}RB* accounts for only 0.8% of FFA loss in the air-saturated solution. The rate of FFA loss in degassed ice is very slow, indicating that $^1O_2$* is the dominant oxidant for FFA in frozen samples: the RB triplet is responsible for only approximately 0.1% of FFA decay in air-saturated ice.

In contrast to the lack of triplet reactivity with aqueous FFA, organic triplets react with both TRP[34,35] and BPA[36,37] in solution. For TRP, degassing suggests that ^{3}RB* is increasingly important as the reaction system becomes more liquid in character: i.e., $k^*_{p,degassed}/k^*_p$ increases from the 0.065 mM TS ice case (where $^1O_2$* appears to dominate TRP loss) to the 6.0 mM TS ice case to liquid (where ^{3}RB* appears to dominate in the degassed sample) (Figure 4). This figure also shows that in the air-saturated samples the RB triplet contributes 0.3% (in 0.065 mM TS ice) to 1.7% (in solution) of the total indirect photochemical loss of TRP. For BPA, ^{3}RB* is the major oxidant in the degassed liquid solution (where degassing does not alter k^*_{BPA}; Figure 4) but is minor in degassed ice, consistent with the idea that BPA is segregated from RB in liquid-like regions in the ice samples. For the air-saturated ice and solution samples, we calculate that ^{3}RB* is a minor sink for BPA, accounting for less than 0.5% of the BPA loss (Figure 4). Overall, while $^1O_2$* is responsible for most of the enhanced loss of pollutants observed on ice, ^{3}RB* makes a minor but noticeable contribution. The triplet contribution is greatest in solution and in ices with higher total solute concentrations, probably because $^1O_2$* is less concentrated under these conditions.

While the ^{3}RB* contribution is small in our air-saturated samples, these results suggest that the steady-state concentration of triplet organic states can be enhanced on ice compared to in solution. For example, ^{3}RB* accounts for nearly 2% of TRP loss in the air-saturated solution and approximately 1% in the air-saturated 6 mM TS ice samples (Figure 4). Although the ^{3}RB* contribution decreases from solution to 6 mM TS ice, the total rate constant for TRP loss increases by a factor of nearly 200 (Figure 3). Thus the pseudo-first order rate constant for reaction of triplet with TRP (i.e., $k_{TRP+3RB*}$[^{3}RB*]) increases by a factor of approximately 100 from solution to 6 mM TS ice, most likely because of a corresponding increase in the triplet concentration. This freeze-concentration enhancement for [^{3}RB*] is smaller than the enhancement of [$^1O_2$*] in the samples (since the relative contribution of the triplet decreases from solution to 6 mM TS; Figure 4). However, the triplet concentration enhancement on ice

has important implications for species that react rapidly with triplet excited states but only slowly with singlet molecular oxygen (such as phenols in neutral or acidic samples). The cause for the triplet enhancement is probably analogous to the case for $^1O_2$*: the concentration of the triplet source (e.g., RB) in LLRs should be increased by a factor of approximately *F*, while the concentration of the dominant sink for the triplet states (i.e., O_2) will be roughly the same as its solution value.[20,21] The end result is that triplet-mediated reactions should be enhanced in/on ice relative to in liquid solution. Additional experimental work needs to be completed to determine the apparent freeze-concentration factors for concentrations of triplet excited states, but given their importance as oxidants in environmental waters and particles,[38,39] it is likely that they are also important in/on ice.

In addition to the degassing controls, we also performed ice experiments using D_2O instead of H_2O as the solvent to examine the significance of $^1O_2$* in our pollutant degradations. This solvent exchange should have a negligible effect on reaction pathways other than $^1O_2$*. But it should increase the steady-state concentration of $^1O_2$* in D_2O by a factor of approximately 14 compared to in H_2O; this is because the solvent is the dominant $^1O_2$* sink and the rate constant for deactivation of $^1O_2$* by H_2O is 13.8 times greater than by D_2O.[9,21] While this diagnostic tool is common in solution studies,[9,14,15] it has been applied only recently to ice samples.[20,21]

In experiments with ice made from 6.0 mM TS solutions, FFA loss is 9 ± 3 times higher in D_2O (Figure 5), consistent with $^1O_2$* being the dominant oxidant, as indicated by the degassing result (Figure 4). Unexpectedly, in the remaining five conditions shown in Figure 5, there is little, if any, enhancement in k^*_p in D_2O compared to in H_2O. For FFA and TRP in 0.065 mM TS the rate constants for loss are actually lower in D_2O compared to in H_2O, with $k^*_{p,D2O}/\ k^*_{p,H2O} < 0.5$. In contrast to the enhanced FFA loss with 6.0 mM TS, TRP loss in D_2O ice with 6.0 mM TS showed very little enhancement, by only a factor of about 1.8 ± 0.6. Along with the degassing experiments, this D_2O result supports the idea that ^{3}RB* is an important oxidant in this system. The results for BPA were opposite to those of FFA and TRP: enhancement was observed (3.9 ± 1.5) in the 0.065 mM D_2O ice, but there was essentially no effect of D_2O in the 6.0 mM TS ice (0.9 ± 0.3).

These seemingly confounding results can be explained by considering the freezing point of D_2O and its rate constant with $^1O_2$*. The freezing point for D_2O is 3.7 ˚C,[40] which suggests that upon freezing D_2O solutions the D_2O crystallizes first, while any H_2O impurity remains unfrozen initially, allowing it to preferentially partition into LLRs. The net result would be a reduction of the expected D_2O enhancement because of preferential H_2O contamination in LLRs. In addition, there are also trace amounts of H_2O in our D_2O solutions because we prepared our RB and pollutant stock solutions in Milli-Q. While we worked to keep the H_2O addition to our D_2O solutions to a minimum, enough H_2O was added that it could affect our results in Figure 5. From the water-based stocks our D_2O solutions contained approximately

0.2% H_2O by volume. In comparison, from Equation 2 we calculate that in ice samples at –10 ˚C with 0.065 mM TS about 0.001% of the initial solvent molecules end up in LLRs; for 6.0 mM TS the percentage is approximately 0.1%. In both cases, the volume of H_2O added to our D_2O stocks is greater than the estimated total volume of LLRs, highlighting the potential importance of trace levels of H_2O.

The other possible reason D_2O-ice samples fail to show an enhancement in pollutant loss relative to H_2O-ice samples is because of differences in the importance of the pollutant as a sink for $^1O_2$* in the two solvents. We chose very low pollutant concentrations so that the pollutant accounts for less than 30% of $^1O_2$* loss in H_2O ices.[20] However, since D_2O is a relatively slow sink for $^1O_2$* compared to H_2O, the pollutant becomes a more important sink for $^1O_2$* in D_2O-ice samples (Supplemental section S4). In H_2O ice (–10˚C, 0.065 mM TS), with our typical pollutant concentrations, H_2O is the dominant sink and the pollutants account for 12 to 29% of $^1O_2$* loss (Supplemental Table S1). In contrast, for otherwise identical solutions prepared in D_2O, the pollutants consume 67 to 85% of $^1O_2$* (Table S1). That is, in each case the pollutant – and not D_2O – is the dominant sink of $^1O_2$* in the D_2O ices. Because of this, in the 0.065 mM TS ices changing the solvent from H_2O to D_2O will have little to no effect on k^*_p. As derived in the Supplemental Material (section S4 and Table S2), we calculate that $k^*_{p,D2O}/\ k^*_{p,H2O}$ ratios should be 0.7 for FFA, 1.5 for TRP, and 2.6 for BPA for the 0.065 mM TS ices. These are similar to the measured $k^*_{p,D2O}/k^*_{p,H2O}$ ratios of 0.4 ± 0.1 for FFA and 3.9 ± 1.5 for BPA (Figure 5). That the calculated values are similar to what we observe for FFA and BPA is consistent with $^1O_2$* being the dominant oxidant in these samples, as suggested by the degassed, 0.065 mM TS ice results (Figure 4). However, the $k^*_{p,D2O}/k^*_{p,H2O}$ ratio of 0.23 ± 0.08 for TRP was lower than expected, which could be further evidence that ^{3}RB* is an important TRP sink in these samples.

For the ices with 6.0 mM TS, the pollutants are all minor sinks for $^1O_2$* in both H_2O and D_2O (Supplemental Table S1) so $k^*_{p,D2O}/\ k^*_{p,H2O}$ should be roughly 14 for these conditions. In this case, enhanced FFA loss in D_2O (Figure 5) implicates $^1O_2$* as the dominant oxidant, a conclusion supported by the degassing results (Figure 4). On the other hand, the low D_2O enhancement for TRP loss in 6.0 mM TS ice (1.8; Figure 5) suggests that $^1O_2$* contributes to TRP loss on ice, but that some other oxidant – likely ^{3}RB* – is also involved. In the case of BPA with 6.0 mM TS the degassing experiments suggest $^1O_2$* is the dominant oxidant but there is no enhancement in k^*_{BPA} in D_2O, arguing against $^1O_2$* as the dominant sink: this is a more complicated picture, possibly related to the low solubility of BPA. This lower observed enhancement could imply aggregation of BPA into organic-microregions within liquid-like regions or the bulk matrix of the ice, as has been reported in liquid solutions of singlet oxygen formation sensitized by natural CDOM.[29]

4. Conclusions

Steady-state concentrations of $^1O_2$* can be greatly enhanced on ice relative to liquid solutions, suggesting that $^1O_2$* can be an important oxidant for certain pollutants on snow and ice. In illuminated ice with Rose Bengal and total solute concentrations in the range of remote, continental snows (0.065 mM), the loss of both furfuryl alcohol and tryptophan is greatly accelerated on ice, by factors approaching 10^4. At higher total solute concentrations (6.0 mM), the rate constants for loss are lower, but still 10^3 times higher for furfuryl alcohol and 100 times higher for tryptophan compared to the liquid values. We also find enhanced loss of bisphenol A on ice, but to a lesser extent, at just 50 times higher than in liquid samples. In only the case of furfuryl alcohol at 6.0 mM total solutes does the experimental enhancement match what is predicted by freezing-point depression. The diminished enhancement of pollutant loss in the other cases could be a result of aggregation or precipitation of sensitizer and/or pollutant. In particular, the least soluble pollutant studied here (bisphenol A) had the least enhancement of ice-phase loss and it was independent of total solute concentration. In natural settings, regions of organic aggregation likely house hydrophobic compounds, including dissolved organic matter that can sensitize $^1O_2$* formation, creating sub-phases where production of $^1O_2$* and subsequent degradation of hydrophobic pollutants may be more important than observed here since we utilized a highly water-soluble sensitizer.

Our results indicate that another oxidant – probably the excited triplet state of Rose Bengal – can also be important in the degradation of certain organic molecules, both in ice and in solution. In deoxygenated ice with 6.0 mM TS, the loss of TRP suggests that ^{3}RB* concentrations are enhanced on ice, though not to the same degree as $^1O_2$*. Although the removal of O_2 leads to artificially high concentrations of ^{3}RB* in the degassed samples compared to the air-saturated samples, the degassed results indicate that triplet state concentrations are enhanced in/on ice compared to in solution. It will require additional work to quantify this enhancement and its dependence on solute concentrations and temperature. While the importance of $^1O_2$*, and perhaps excited triplet states of natural organic matter, as sinks for ice-phase organics depends on a number of factors – such as the collocation of sensitizers and pollutants – our results suggest that $^1O_2$* and triplet states probably play important roles in the transformations of certain classes of organic molecules in illuminated snow and ice.

Acknowledgements

This research was supported by funding from the National Science Foundation (grant CHE-1214121) and a graduate fellowship (grant # FP916999) to J.B. from the U.S. Environmental Protection Agency's Science to Achieve Results (STAR) program. Although the research described in the article has been funded wholly or in part by the U.S. EPA, it has not been subject to any EPA review and therefore does

not necessarily reflect the views of the Agency, and no official endorsement should be inferred. We thank Harry Beine, Bill Casey, and two anonymous reviewers for comments that improved the manuscript.

References

(1) Kahan, T. F.; Donaldson, D. J., *J. Phys. Chem. A*, 2007, **111**, 1277-1285.
(2) Ram, K.; Anastasio, C., *Atmos. Environ.*, 2009, **43**, 2252-2259.
(3) Matykiewiczova, N.; Klanova, J.; Klan, P., *Environmental Science & Technology*, 2007, **41**, 8308-8314.
(4) Klanova, J.; Klan, P.; Nosek, J.; Holoubek, I., *Environ. Sci. Technol.*, 2003, **37**, 1568-1574.
(5) Weber, J.; Kurková, R.; Klánová, J.; Klán, P.; Halsall, C. J., *Environ. Pollut.*, 2009, **157**, 3308-3313.
(6) Anastasio, C.; Galbavy, E. S.; Hutterli, M. A.; Burkhart, J. F.; Friel, D. K., *Atmos. Environ.*, 2007, **41**, 5110-5121.
(7) Chu, L.; Anastasio, C., *J. Phys. Chem. A*, 2005, **109**, 6264-6271.
(8) France, J. L.; King, M. D.; Lee-Taylor, J., *Atmos. Environ.*, 2007, **41**, 5502-5509.
(9) Bilski, P.; Holt, R. N.; Chignell, C. F., *J. Photochem. Photobiol. A*, 1997, **109**, 243-249.
(10) Haag, W. R.; Hoigne, J.; Gassman, E.; Braun, A. M., *Chemosphere*, 1984, **13**, 631-640.
(11) Wayne, R. P., *Res. Chem. Intermed.*, 1994, **20**, 395-422.
(12) Muraseccosuardi, P.; Gassmann, E.; Braun, A. M.; Oliveros, E., *Helv. Chim. Acta*, 1987, **70**, 1760-1773.
(13) Zepp, R. G.; Wolfe, N. L.; Baughman, G. L.; Hollis, R. C., *Nature*, 1977, **267**, 421-423.
(14) Anastasio, C.; McGregor, K. G., *Atmos. Environ.*, 2001, **35**, 1079-1089.
(15) Faust, B. C.; Allen, J. M., *J. Geo. Res.*, 1992, **97**, 12913-12926.
(16) Boreen, A. L.; Edhlund, B. L.; Cotner, J. B.; McNeill, K., *Environ. Sci. Technol.*, 2008, **42**, 5492-5498.
(17) McGregor, K. G.; Anastasio, C., *Atmos. Environ.*, 2001, **35**, 1091-1104.
(18) Han, S. K.; Bilski, P.; Karriker, B.; Sik, R. H.; Chignell, C. F., *Environ. Sci. Technol.*, 2008, **42**, 166-172.
(19) Tratnyek, P. G.; Hoigne, J., *J. Photochem. Photobiol. A*, 1994, **84**, 153-160.
(20) Bower, J.; Anastasio, C., *Journal of Atmospheric Chemistry A*, 2013, **117**, 6612-6621.
(21) Bower, J.; Anastasio, C., *Atmos. Environ.*, 2013, **75**, 188-195.
(22) Anastasio, C.; Robles, T., *Journal of Geophysical Research: Atmospheres*, 2007, **112**, D24304.
(23) Galbavy, E. S.; Ram, K.; Anastasio, C., *J. Photochem. Photobiol. A*, 2010, **209**, 186-192.
(24) Datta, A.; Chatterjee, S.; Sinha, A. K.; Bhattacharyya, S. N.; Saha, A., *J. Lumin.*, 2006, **121**, 553-560.
(25) Zhan, M., *Journal of Environmental Sciences*, 2009, **21**, 303-306.
(26) Kahan, T. F.; Donaldson, D. J., *Environ. Sci. Technol.*, 2010, **44**, 3819-3824.
(27) Cho, H.; Shepson, P. B.; Barrie, L. A.; Cowin, J. P.; Zaveri, R., *J. Phys. Chem. B*, 2002, **106**, 11226-11232.
(28) Haynes, W. M., Ed. Cryoscopic constants for calculation of freezing point depression. In *Handbook of Chemistry and Physics, 92nd Edition, Internet Version*; CRC Press/Taylor and Francis: Boca Raton, FL, 2012.
(29) Latch, D. E.; McNeill, K., *Science*, 2006, **311**, 1743-1747.
(30) Douglas, P.; Waechter, G.; Mills, A., *Photochem. Photobiol.*, 1990, **52**, 473-479.
(31) Iu, K. K.; Ogilby, P. R., *J. Phys. Chem.*, 1987, **91**, 1611-1617.
(32) Shimizu, O.; Watanabe, J.; Naito, S.; Shibata, Y., *J. Phys. Chem. A*, 2006, **110**, 1735-1739.
(33) Halladja, S.; ter Halle, A.; Aguer, J.-P.; Boulkamh, A.; Richard, C., *Environ. Sci. Technol.*, 2007, **41**, 6066-6073.
(34) Muszkat, K. A.; Wismontski-Knittel, T., *Biochemistry*, 1985, **24**, 5416-5421.

(35) Tsentalovich, Y. P.; Morozova, O. B.; Yurkovskaya, A. V.; Hore, P. J., *The Journal of Physical Chemistry A*, 1999, **103**, 5362-5368.
(36) Anastasio, C.; Faust, B. C.; Rao, C. J., *Environ. Sci. Technol.*, 1997, **31**, 218-232.
(37) Golanoski, K. S.; Fang, S.; Del Vecchio, R.; Blough, N. V., *Environ. Sci. Technol.*, 2012, **46**, 3912-3920.
(38) Canonica, S.; Jans, U.; Stemmler, K.; Hoigne, J., *Environ. Sci. Technol.*, 1995, **29**, 1822-1831.
(39) Zepp, R. G.; Schlotzhauer, P. F.; Sink, R. M., *Environ. Sci. Technol.*, 1985, **19**, 74-81.
(40) Smirnova, N. N.; Bykova, T. A.; Van Durme, K.; Van Mele, B., *J. Chem. Thermodyn.*, 2006, **38**, 879-883.
(41) Gottfried, V.; Kimel, S., *Journal of Photochemistry and Photobiology B-Biology*, 1991, **8**, 419-430.
(42) Barbieri, Y.; Massad, W. A.; Díaz, D. J.; Sanz, J.; Amat-Guerri, F.; García, N. A., *Chemosphere*, 2008, **73**, 564-571.
(43) Acros Organics, 2009.
(44) Merck, 2007.
(45) Alfa Aesar. Bisphenol A MSDS No. A10324; Alfa Aesar, A Johnson Matthey Company: Ward Hill, MA, Accessed at www.ucmsds.com (Accessed on October 28, 2012). 2011.

Tables:

Table 1: Second-order rate constants (k_{p+1O2*}) and water solubilities for the three representative pollutants.

	Furfuryl Alcohol (FFA)	Tryptophan (TRP)	Bisphenol A (BPA)
Chemical Formula	$C_5H_6O_2$	$C_{11}H_{12}N_2O_2$	$C_{15}H_{16}O_2$
$k_{p + 1O2*}$, $M^{-1}s^{-1}$ (298 K)[a]	1.2×10^8	5.9×10^7	1.0×10^8
$k_{p + 1O2*}$, $M^{-1}s^{-1}$ (263 K)[b]	4.1×10^7	2.6×10^7	4.3×10^7
Solubility in Water[c]	Miscible	56 mM	0.53 mM
Structure	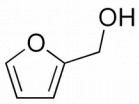	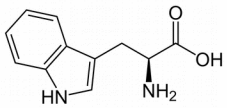	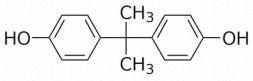

[a]Rate constants for reaction of *p* with $^1O_2$* in water. Values for FFA and TRP are from Gottfried and Kimel[41] and the BPA value is from Barbieri et al[42].
[b]Rate constants at 263 K were determined using E_a values from Gottfried and Kimel[41] for FFA (22.7 kJ m^{-1} K^{-1}) and TRP (15.9 kJ m^{-1} K^{-1}); E_a for BPA was assumed to be the same as for TRP.
[c]Room temperature values from material safety data sheets for FFA [43], TRP [44], and BPA [45].

Scheme 1: Excitation and fate of chromophoric dissolved organic matter (CDOM) in experimental solutions.

Figures:

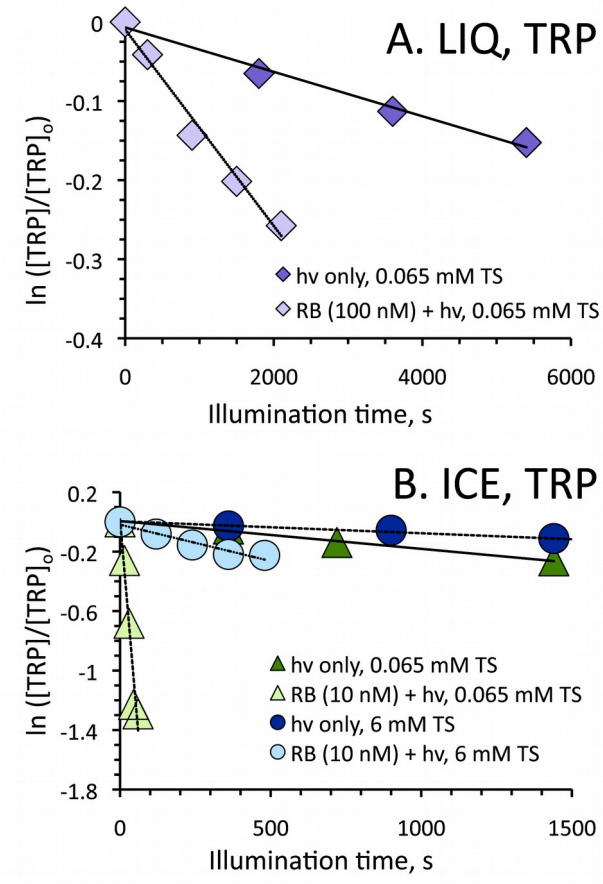

Figure 1. Loss of tryptophan (TRP) in liquid (A; 5˚C) and ice (B; –10˚C) samples both with an added sensitizer for $^1O_2$* (RB + h*v*) and without (h*v* only). All samples were illuminated with 549 nm light. Data for the regression lines are given in Supplemental Material, section S2.

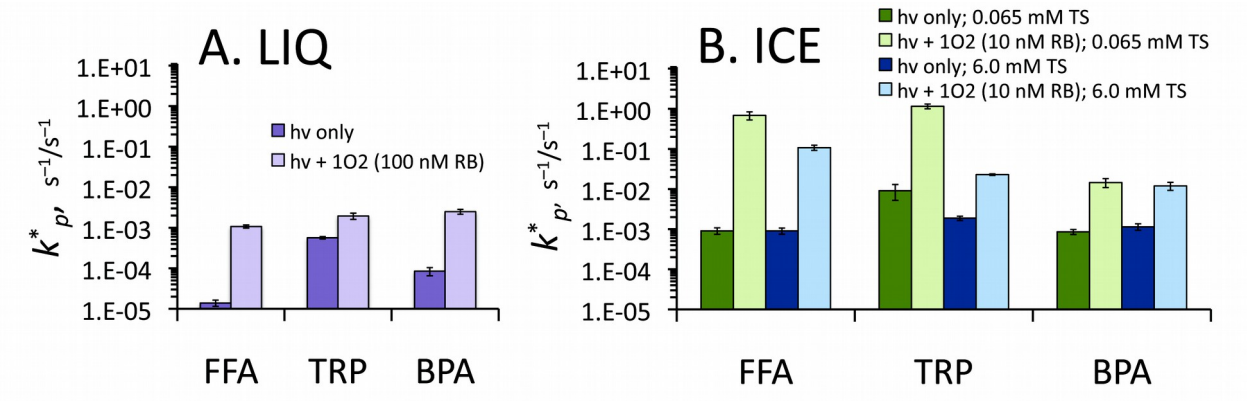

Figure 2. Photon-flux-normalized, pseudo-first-order rate constants for loss of pollutants (k^*_p, for p = FFA, TRP, or BPA) in liquid (A; 5˚C) and in/on ice (B; –10˚C) with an added sensitizer for $^1O_2$* (RB + hν) and without (hν only). Sensitizer (RB) concentrations were 100 nM for liquid and 10 nM for ice; all samples were illuminated with 549 nm light. The total solute concentration in liquid solutions was 0.065 mM (primarily from NaCl), while the ice samples were made from solutions containing 0.065 and 6.0 mM TS using NaCl. Errors bars here, and in subsequent figures, represent ± 1 standard error, propagated from the standard errors of the measurements.

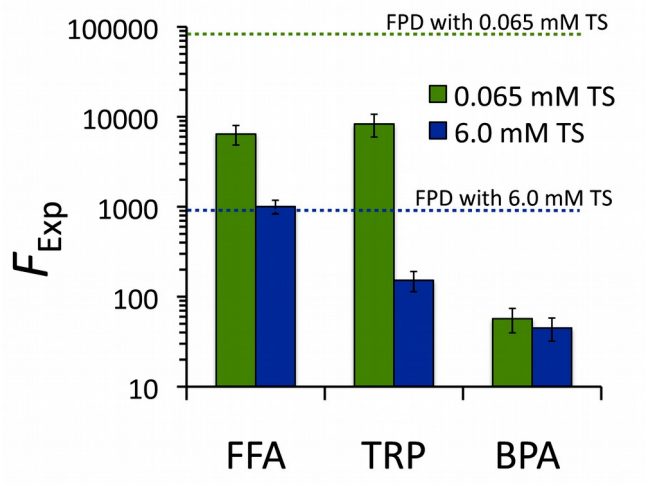

Figure 3. Enhancement of pollutant loss on ice, as shown by the freeze concentration factor (F_{Exp}) determined from measured rate constants for pollutant loss in ice (–10˚C) and in solution (5˚C) (Equation 3). The dashed lines show calculated values of F from freezing-point depression (FPD) at –10˚C.

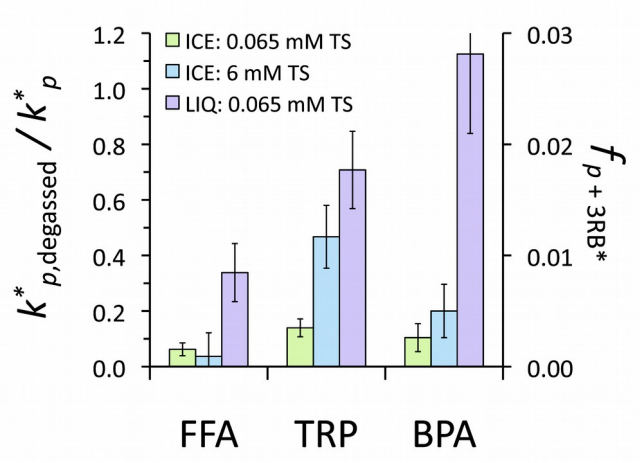

Figure 4. Effect of degassing on the rate constant for loss of pollutant in illuminated liquid (5˚C) and ice (–10˚C) samples containing RB. The left-hand y-axis represents the ratio of k^*_p observed in degassed samples ($k^*_{p,degassed}$) to that observed in samples made from air-saturated solutions (k^*_p). A value of 1 represents no effect from degassing, while values below 1 indicate a sensitivity to O_2, presumably because $^1O_2$* is a significant oxidant in the air-saturated sample. The right-hand y-axis shows the approximate fraction of pollutant degradation due to ^{3}RB* (f_{p+3RB}) in the air-saturated sample. Note that the relationship between the y-axes is only linear at small values of f_{p+3RB}.

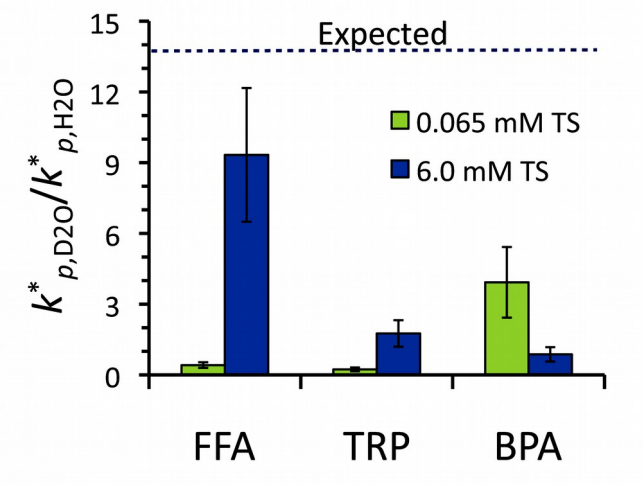

Figure 5. The effect of D_2O on the degradation of pollutants in illuminated ice (–10˚C) containing RB, shown as the ratio of k^*_p in ices made with D_2O to k^*_p in ices made with H_2O. For aqueous pollutants whose major sink is $^1O_2$* we expect k^*_p in D_2O to be enhanced by a factor of 13.8 relative to in H_2O (dotted line).